

Experimental Study on Corrosion, Mechanical and Wear Properties of Nano-ZrO₂ Doped Aluminum Composite

**K.S. Harishanand¹, H. Nagabhushana², B.M. Nagabhushana³,
M.M. Benal⁴, M S Muruli⁵, N Raghavendra¹,
and K R Vishnu Mahesh⁶**

¹*Department of Mechanical Engineering, R.V. College of Engineering
Bengaluru-560059, India*

²*Department of Physics, Tumkur University, Tumkur-572103, India*

³*Department of Chemistry, M.S. Ramiah Institute of Technology
Bengaluru-560054, India*

⁴*Department of Mechanical Engineering, Govt. Engineering College
Kushalnagar-571234, India*

⁵*Dronacharya Group of Institutions, Greater Noida, UP, India*

⁶*Department of Chemistry, ACS College of Engineering
Bengaluru-560074, India*

Abstract

Zirconil Oxide (ZrO₂) Nano powder produced by solution combustion synthesis (SCS) at 500 ± 10°C temperature using fuel as ODH (Oxalyl di hydrazide) solution. The obtained ZrO₂ powder was characterized by XRD, SEM and EDX. The powder blends of ZrO₂/Al were prepared by low energy ball milling and the composite blocks of ZrO₂/Al were fabricated by pressing the powder mix in a sophisticated dye using hydraulic press then sintered at 550° C for 45 Minutes in an inert atmosphere of organ gas. The micro-hardness, wear resistance and corrosion resistance of ZrO₂/al blocks were studied. The results showed that the micro-hardness, wear resistance and corrosion resistance improved significantly with addition of ZrO₂ nano powder up to 1 wt % and increase in ZrO₂ % only decreased the values of all the desirable properties. The optimal micro hardness and microstructure are obtained when the mass fraction of ZrO₂ is 1.0% whereas sample with 5wt% of ZrO₂ showed best wear resistance. Corrosion tests reveal that there slight mass loss due to corrosion.

Keywords: ZrO₂, Micro-hardness, Wear resistance and Corrosion resistance.

1. Introduction

High strength aluminium alloys are commonly used in aerospace, transportation, armory and marine industries applications after appropriate corrosion control measures. The corrosion mechanisms of aluminium alloy have been extensively studied and protection treatments developed [1–7]. They relatively resist corrosion when exposed to various aggressive environments. These environments may include water vapour, acid and base solutions. Most of these environments degrade the quality of the aluminum and its alloys and affects the mechanical properties of the system thereby reducing their life-span [8-10].

For many years, materials researchers have been keenly interested in ceramics nanopowders due to their optimum sintering and mechanical properties [11]. Furthermore, composites with nanograins have several advantages in that they possess improved properties, such as corrosion resistance, mechanical, electrical, thermal, ionic conducting, catalytic, and optical properties [12].

Zirconia, ZrO₂, is considered nowadays one of the most important ceramic materials in modern technology [13-14]. It has a wide range of industrial applications because of the excellent combination of high flexural strength (~1 GPa) and good fracture toughness (~10 MPa m^{1/2}), together with its stability at high temperature and its optimal dielectric constant (ε₀) of around 20 [15]. It is used for metal coatings, as a refractory material in insulation, abrasives, enamels and glazes, as support material for catalysis [16-21] and, due to its ion conductivity, it is also applied in gas sensors [22], oxygen pumps for partial pressure regulation [13, 23] and high temperature fuel cells [24]. Further, ZrO₂ is one of the most radiation-resistant ceramics currently known [25-26] and therefore has a particular importance in the nuclear industry. Recently, together with hafnia, it has been proposed to substitute SiO₂ as a gate dielectric material in metal-oxide semiconductor devices [27-28].

Among the available ceramic nanoparticles, zirconia appears to be one of the most promising materials and has long found use in coating technology due to its high strength, fracture toughness, chemical durability, thermal stability, high refractive index and low optical absorption [29-33]. Zirconia possesses several crystal structures at different temperatures, since it is a polymorphic material. With control of the martensitic transformation and grain size, one can design desired properties of zirconia for a specific coating application. Hence, the combination of PPy and zirconia could be the most desirable for application to orthopaedic implants exposed to high friction and high impact due to the promising mechanical properties such as high fracture toughness and hardness as well as bioinertness of the zirconia component [33-37].

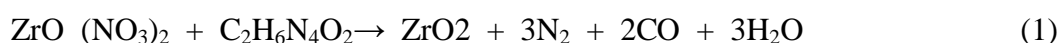
Due to the enormous technological significance of metal/zirconia systems, there has been a great effort to fabricate metal/zirconia-based materials with

controlled structure and properties. Since many properties are intimately related to the existence of good and strong metal–zirconia interfaces, many investigations are devoted not only to the production of the heterogenous materials but also to control the interface between them. From the open literature [1-37] the ZrO₂ based aluminum composites were attracted much attention in various applications hence in this work, the nano-ZrO₂/Al powder blends were used to prepare ZrO₂/Al blocks by cold pressing followed by sintering, and the performance of the fabricated blocks were studied for hardness, wear resistance and corrosion resistance.

2. Experimental

2.1. Synthesis of ZrO₂ powder

The ZrO₂ nano powder was prepared by dissolving zinc nitrate (Zr (NO₃)₂ · 6 H₂O) and ODH (Oxalyl di hydrazide) solution as fuel in a minimum quantity of double distilled water is taken in a Pyrex dish. The dish containing the solution was introduced into a pre-heated muffle furnace maintained at 500 ± 10° C. The solution initially boils and undergoes dehydration followed by decomposition with the evolution of large amount of gases. At the point of spontaneous combustion, the solution begins burning and releases lot of heat; all the solution vaporizes instantly and becomes a burning solid. The entire combustion process for producing ZrO₂ powder takes place. The reaction for combustion synthesis in the present case can be written as equation (1):



2.2. Preparation of ZrO₂/Al powder blends and ZrO₂/Al blocks

After the combustion process obtained nano ZrO₂ powder was added to commercially available pure 99.5% aluminum powder. The ZrO₂ powder was mixed with an increment of 0.25, 0.5, 1, 2.5 and 5 wt% were mixed for 30 minutes by hand mixing and loaded in metal die for compaction. The powder metallurgy technique was used to fabricate the ZrO₂ doped Al blocks. Powder blends were cold pressed at 200 Mpa to approximately 90 % compression and then sintered at 500° C for 1hour. The sintered ZrO₂/Al blocks were polished with fine emery papers with grit size ranging from 200 to 2000 followed by diamond paste polishing for obtaining mirror finish surface on the specimen blocks.

2.3. XRD, Surface Morphology, EDX and Microstructures of ZrO₂ and ZrO₂/Al blocks

X-ray Diffractometer (XRD: Shimadzu 700 S, Japan), Scanning Electron Microscopy (SEM: JEOL, Japan, JSM 840A) were employed to analyze the powder and morphology of the ZrO₂ powder and polished surfaces of ZrO₂/Al blocks. The grain size and microstructure was studied using optical microscope.

2.4. Micro-hardness test.

Micro hardness was tested using Vickers Micro-hardness tester with diamond indenter in the form of right pyramid and a square base. An optical microscope with up to 400X magnification along with a Micrometer attachment in the eye piece was used to observe and measure the length of the diagonal of indentation. Microscope attachment helps in determining the distribution of ZrO₂ dopant in the samples doped at different percentages.

2.5. Corrosion resistance test

Two separate tests were performed to evaluate the corrosion resistance of the ZrO₂/Al blocks. The specimens were soaked in the spray tank with 3.5% NaCl solution for 50 hr and then were rinsed, dried and weighed. The corrosion resistance was evaluated by the mass loss per area, $\Delta m/S$ (Δm is the mass loss and S is the surface area). The specimens were soaked in the spray tank with 0.5 mol MgSO₄ solution for 10 hr and then were rinsed, dried and weighed.

2.6. Wear resistance test.

Pin on disc apparatus was used to measure the wear resistance of the samples. ZrO₂/Al samples of size 10×10×20 mm³ were fabricated and mounted on pin on disk apparatus and made to rub against the rotating stainless steel disk. Area exposed to wear was 10×10 mm². Relative velocity of wear test sample with respect to the rotating disk was 2.6 ms⁻¹ and sliding distance was 1.6 km. Mass loss due to wear was calculated for each samples of variant wt % of dopants after completion of wear test.

3. Results and Discussion

3. 1 X-ray Diffractometer (XRD) Studies

The X-ray diffraction pattern of nano-ZrO₂ powder confirms the crystalline phase and mean crystal size determined was around 40 nm. In the XRD observations three strongest peaks shown in Fig.1. were detected with Miller indices (1 0 0), (0 2 0), (200), (111), (201), (031), (002), (040) and (231) corresponding to Bragg angles 24°, 28°, 31°, 35°, 41°, 50°, 54°, 55° and 60° respectively. The characteristic peaks are higher in intensity which indicates that the products are of good crystalline nature. No peaks corresponding to impurities are detected, showing that the final product is purely ZrO₂. It is observed that intensity of the peaks increases with thermal treatment due to agglomeration, which means that the crystallinity has been improved. The full width at half maxima of major peaks decreases and confirms the grain size growth.

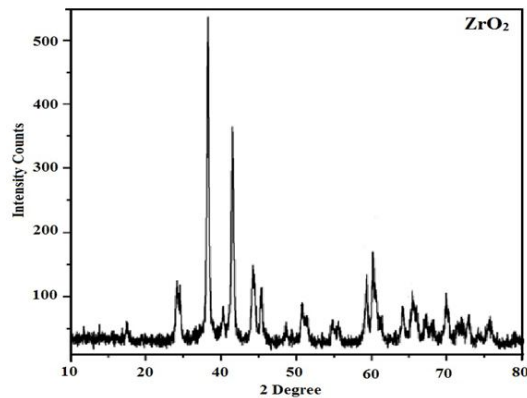


Fig.1. XRD Patron of bare ZrO₂ nanopowder

The XRD of ZrO₂ dispersed in aluminum powder shown in Fig.2 in increment with 0.5, 1, 2.5 and 5 wt % are taken to analyze the ZrO₂/al blends, in the X-ray diffractogram showed in the all XRD was same peaks corresponds to ZrO₂ content but the intensity peaks are shifted to very high intensity this was because of the metal content of the blends. There was no much difference was observed in the all blends ranging from 0.5 to 5 wt % which was confirmed the proper mixing and no impurity peaks are observed in XRD.

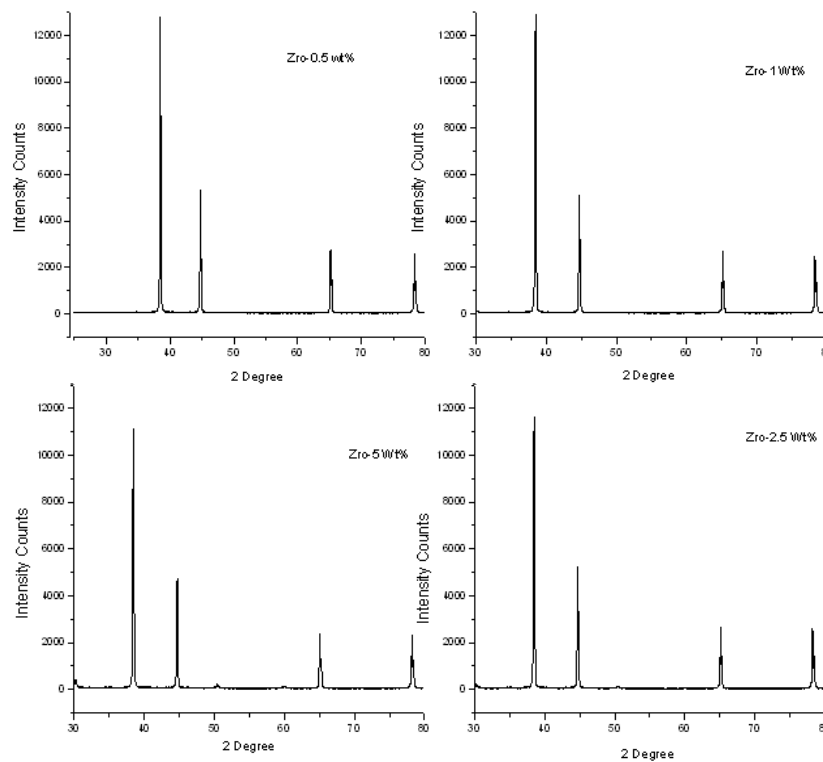


Fig.2. XRD Patron of ZrO₂ doped aluminium blends

3.2. Morphological study using SEM and Elemental composition using EDX of ZrO₂/Al

The nano particulates were found to be agglomerated when analyzed by scanning electron microscopy (SEM) studies shown in Fig.3. This is due to the high surface energy of the particles and from the SEM there is no such difference was observed for different wt % of ZrO₂ dispersed aluminum powder. In micrographs also observing that the big particles are aluminum powder and the very small particles surrounded by that are ZrO₂.

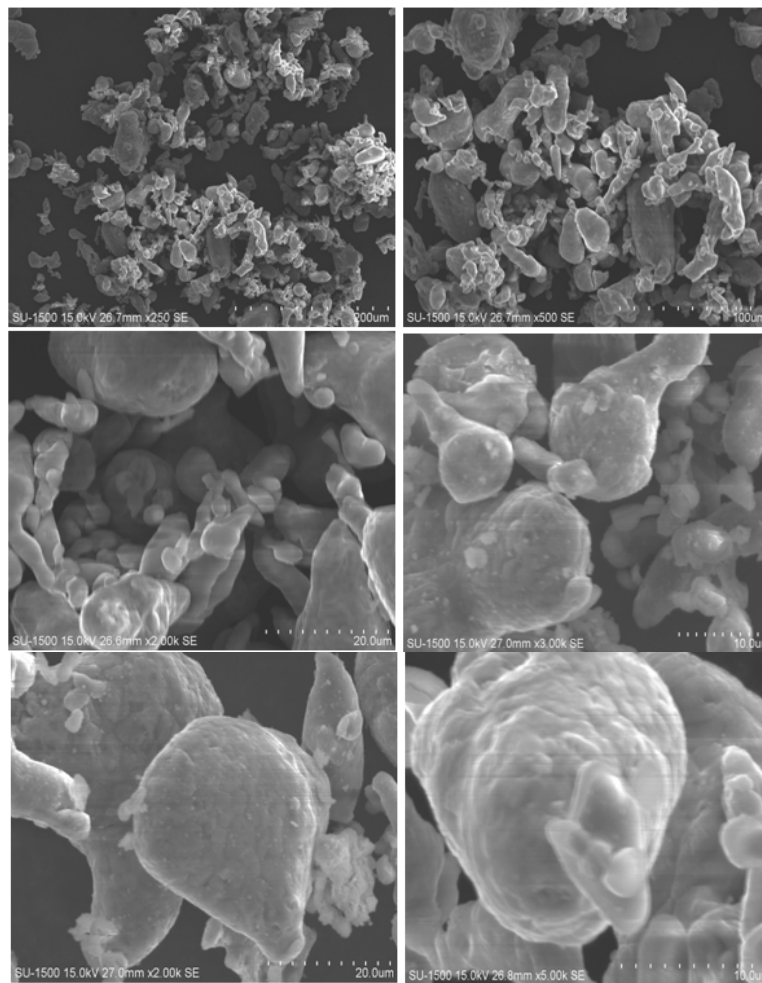


Fig.3. SEM micrographs of ZrO₂ doped aluminum blends

From the EDX Spectrum Fig.4. show very small peaks of ZrO₂ and relatively high peak for aluminum hence it confirms the percentage of the material and also EDX spectrum reveals only the presence of aluminum and ZrO₂ elements and the presence of no other elements was found. Therefore it can be stated that the physical and mechanical parameters are only the attribution of the said two elements in the composition.

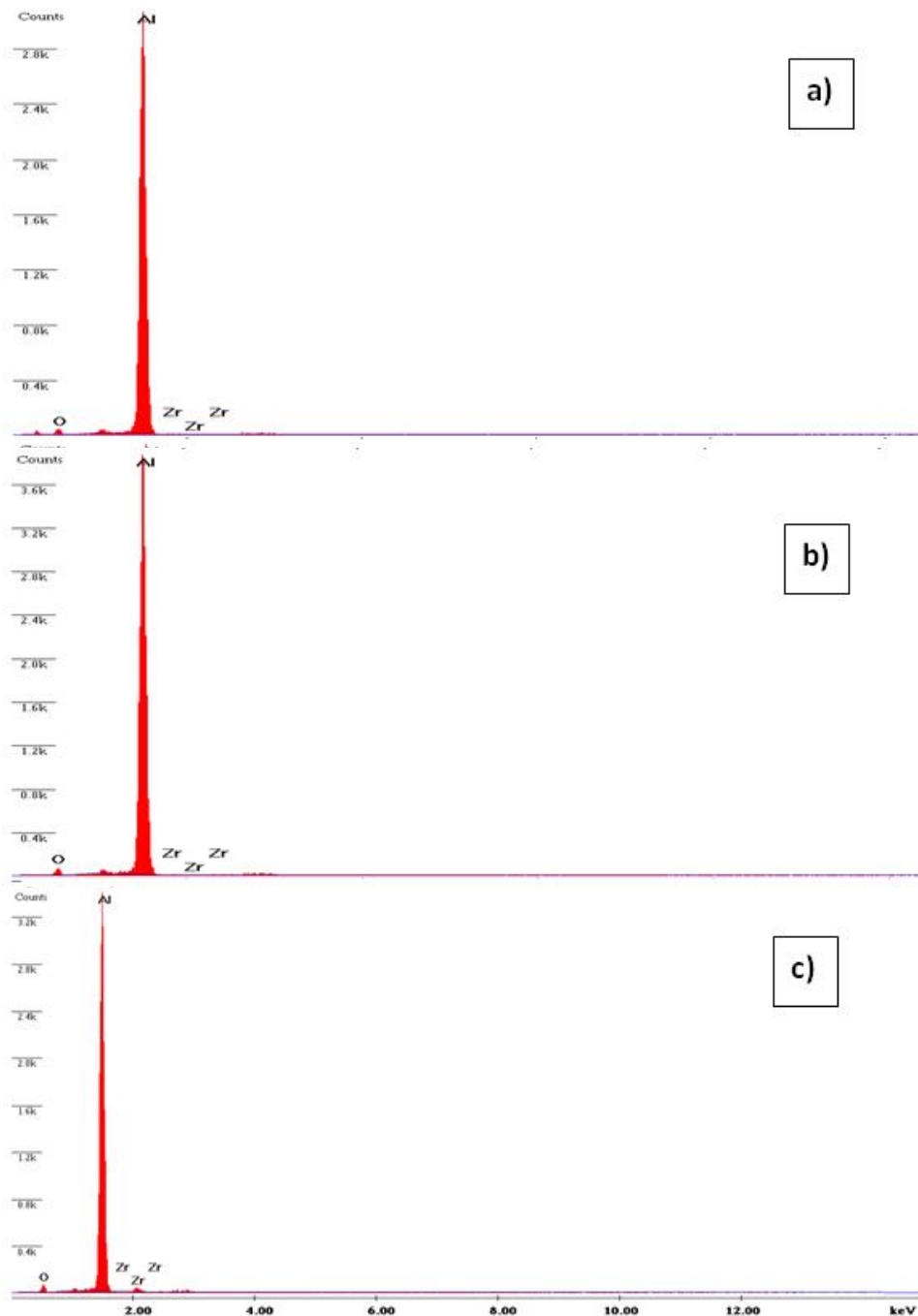


Fig.4. EDX of ZrO₂ doped aluminum blends a) 0.25 %, 1 % and c) 5 % O)

3.3. Micro-hardness or Vickers hardness test

Hardness of a material is defined as the resistance to deformation, particularly permanent deformation, indentation or scratching. Vickers hardness value increased by 7.42, 9.05, 26.96, 24.89 and 21 % with the addition of ZrO₂ in 0.25, 0.5, 1, 2.5 and 5 wt% respectively to aluminum as shown in Fig.5. The

Microhardness of ZrO₂ doped aluminum blocks represents a slow incremental trend in its hardness value with small fractional % dopant inclusion at 0.25 wt % and 0.5 wt %. At 1wt % inclusion of ZrO₂ inclusion as dopant dopant, a sharp rise in hardness value of the block is recorded. Further inclusion of 2.5 wt% and 5 wt % of dopant to the substrate though let to the drop to the microhardness but very close to the value at 1 wt % inclusion of dopant. The graph curve drawn for microhardness to the wt % dopant inclusion remained almost flat but slightly less than the value at 1 wt %. This favor the argument that 1 wt % ZrO₂ dopant is the optimal value at which a maximum hardness of the aluminum block can be produced and beyond 1 wt % is only to decrease in density of the block with an compromise on hardness marginally.

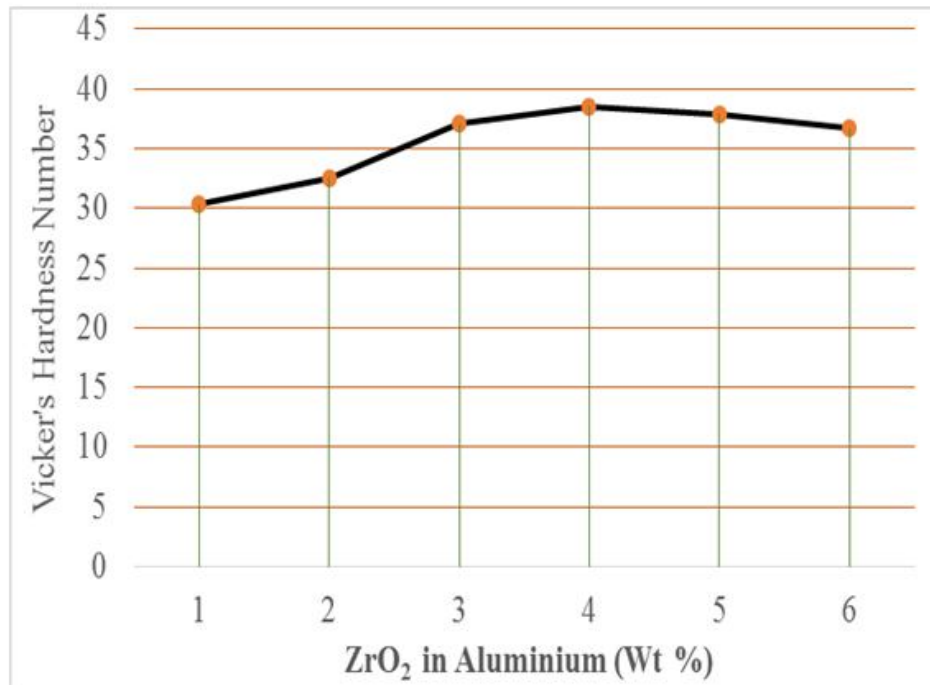


Fig.5. Vickers hardnes of ZrO₂ doped aluminum blends

3.4. Corrosion resistance test

The corrosion characteristic of the aluminum with its variant percentage ZrO₂ do pant matrix is found out independently using standard NaCl and MgSO₄ solutions. It is observed that both solutions has a different influence on the matrix.

In NaCl solution, the matrix instantly drifts to its protection from corrosion by dispersing a small percent of ZrO₂ as do pant. Table.1. shows the further increment in do pant percent has a marginal influence to protect the matrix and the characteristic curve will have a thin slope on increased do pant percentage in the matrix (0.05%-5.0%).

Table 1. ZrO₂/Al composite blocks after corrosion of 40 hours with 3.5% NaCl solution

Sl. No	Wt% of ZrO ₂ doped Al Blocks	Initial weight(gm)	Final weight(gm)	Weight loss in gms	% of corrosion
1	0	23.7861	23.5392	0.2469	1.0380
2	0.25	24.0780	23.9924	0.0856	0.3555
3	0.5	24.0950	24.0421	0.0529	0.2195
4	1.0	25.0362	25.0149	0.0213	0.0850
5	2.5	25.0790	25.0567	0.0223	0.0889
6	5	25.1374	52.1276	0.0098	0.03898

The MgSO₄ solution has a different influence on the do pant percentage as Tabulated in Table. 2. At lower ZrO₂ do pant percentage (0.25%-0.5%) the corrosive property stands almost flat at (0.84%-0.786%). At 1wt% ZrO₂do pant the matrix is highly protected from the corrosion to fall at 0.2306 percent. Beyond 1wt% ZrO₂ do pant the matrix don't show any significant reduction in corrosion protection and hence the characteristic curve exhibit flatness thereafter.

Table 2 ZrO₂/Al composite blocks after corrosion of 10 hours with 0.5M solution of MgSO₄

Sl. No	Wt% of ZrO ₂ doped Al Blocks	Initial weight(gm)	Final weight(gm)	Weight loss in gms	% of corrosion
1	0	15.6381	15.5024	0.1357	0.86
2	0.25	15.6823	15.5491	0.1332	0.84
3	0.5	16.1414	16.1413	0.1270	0.786
4	1.0	16.4324	16.3943	0.0379	0.2306
5	2.5	16.8109	16.7753	0.0356	0.2117
6	5	17.0278	17.0183	0.0095	0.0557

3.5. Wear resistance test

The wear resistance property of the host matrix aluminum exhibit the wavy trend on the pin on disc testing set up. Initially, with just 0.25 wt% do pant the wear drops from 6.0589% to 3.3083% accounting to increase in resistance to wear by 45.39% and further decreasing trend till 1wt% is shown in Table.3. The table listing show least wear at 1wt% of do pant is very significant and is due to the very uniform distribution and super facial bonding of the substrate. Surprisingly the wear resistance decreases by increasing the wt % of do pant from 1wt % to 2.5%.

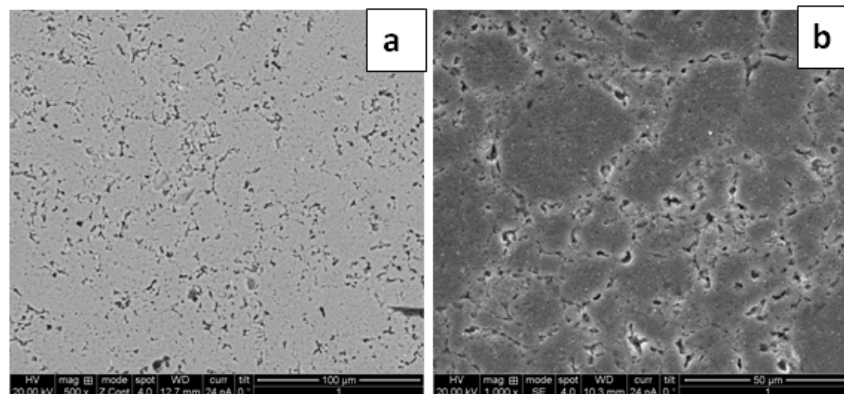
Table 3 Weight loss in samples after wear test to ZrO₂/Al composite blocks

Sl. No	Wt% of ZrO ₂ doped Al Blocks	0 %	0.25 %	0.5 %	1 %	2.5 %	5 %
1	Initial Weight (gm)	4.9365	6.012	6.7981	6.8214	6.9381	6.9908
2	Final Weight (gm)	4.6374	5.8131	6.624	6.6958	6.8105	6.938
3	Weight Loss (gm)	0.2991	0.1989	0.1741	0.0756	0.1276	0.0528
	% of Wear loss	6.0589	3.3083	2.5610	1.1095	0.18391	0.7552

The calculation reads a drop in wear resistance by 60%. This can be attributed to a senior agglomeration of the nano ZrO₂ particle beyond 1wt % and is clearly visible in the SEM images. By increasing the do pant to 5wt% despite agglomeration enhances the wear resistance and trend changes resulting only a .7552% wear Agglomeration of ZrO₂ seen on the entire surface of the substrate and it can be attributed that the ZrO₂ has a property that resists the wear.

3.6 Surface Morphology studies using Microstructures and SEM

The Fig.6 and Fig.7 shows micro structures and SEM images respectively. ZrO₂ particles can be seen well embedded in the grains of aluminum matrix shown as a result of which the structure becomes closer and grains compact. ZrO₂ nano particles are uniformly distributed in Al matrix in case of lower wt % of dopant up to 1 wt % and slight agglomeration of ZrO₂ cannot be seen in major part of the Al matrix as shown. This reveals that the sample has uniform structure and steady performance at doping percentages less than 1 %. At higher doping percentages (2.5% and 5%), agglomeration of ZrO₂ is more common in the aluminum matrix and the ZrO₂ particles are not evenly distributed as shown. This uneven distribution and agglomeration of ZrO₂ in the Al-matrix leads to density variations from one region of the matrix to another. The presence of nano particles in the grain boundaries was the cause for suppression of non-columbic loss of the grains and hence self-corrosion. Almost similar observations were made on the SEM micrographs of the other samples containing different wt % of ZrO₂ in aluminum.



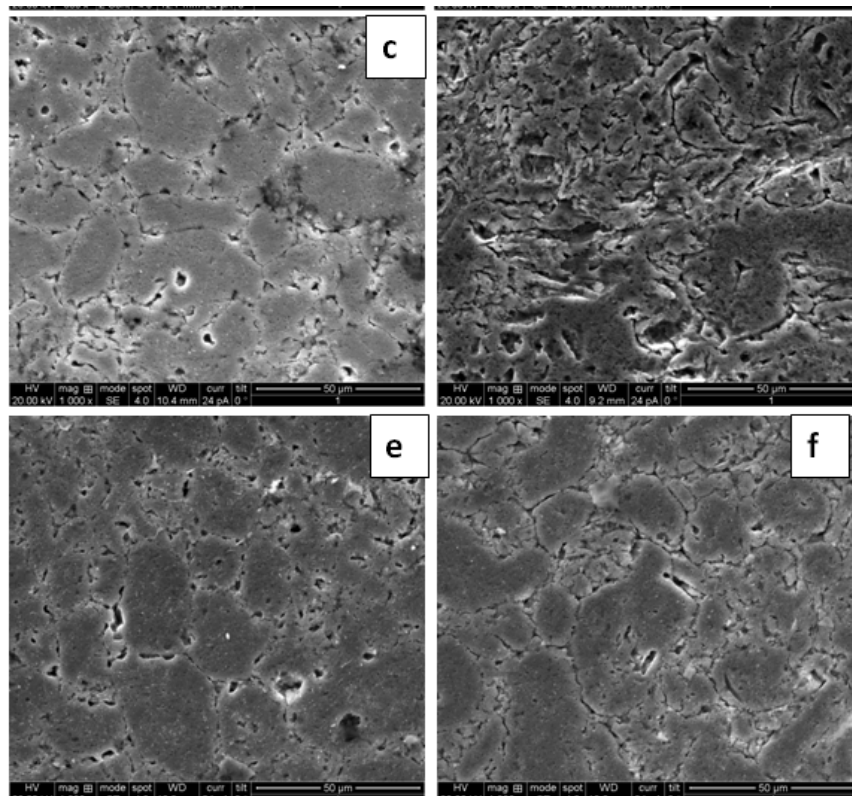
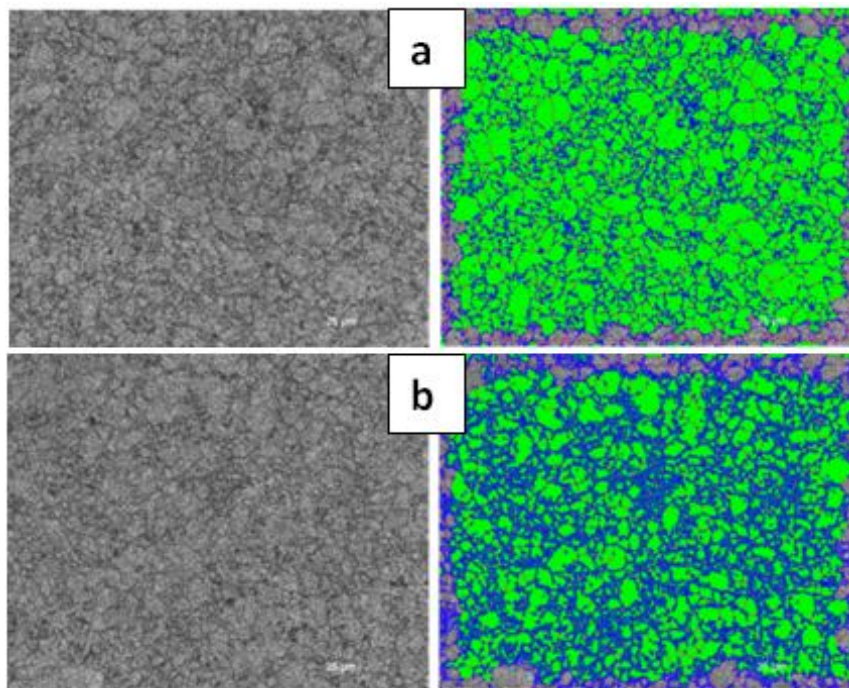


Fig.6. SEM micrographs of ZrO₂ doped aluminum blends a) 0 %, b) 0.25 % c) 0.5 %, d) 1 % e) 2.5 % and f) 5 %



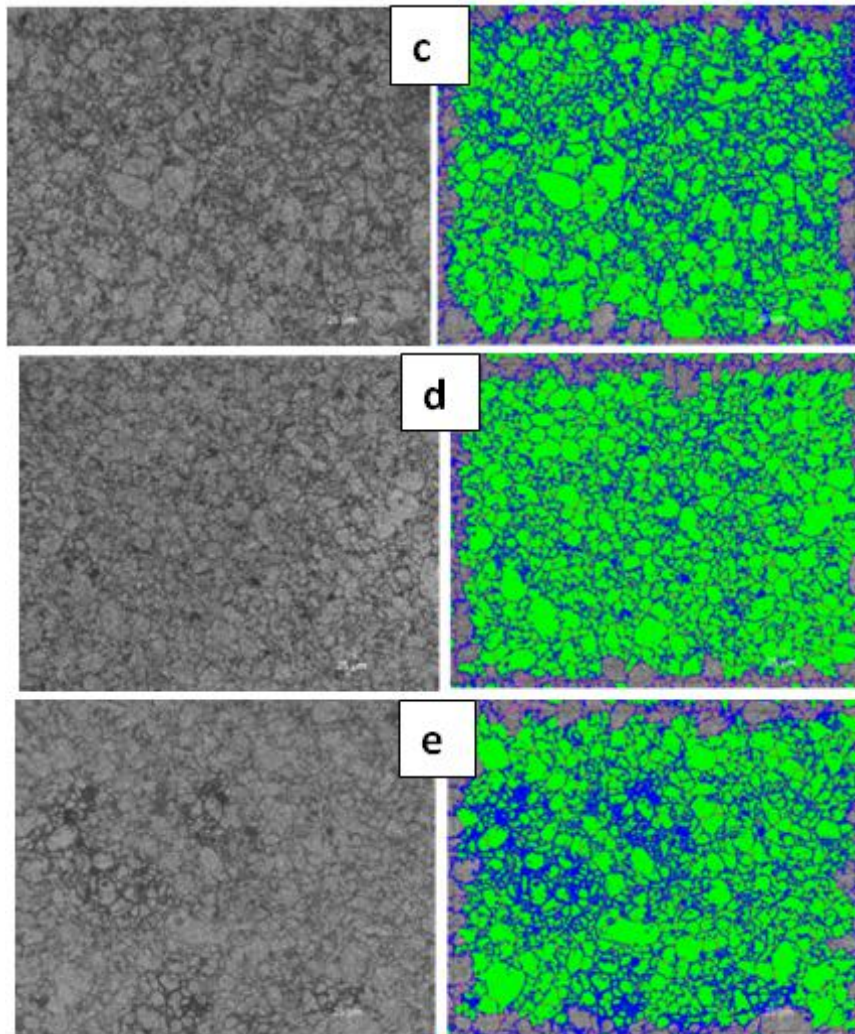


Fig.7. Micrographs micrographs of ZrO₂ doped aluminum blends a) 0 %, b) 0.25 % c) 0.5 %, d) 1 % e) 2.5 % and f) 5 %

4. Conclusion

In the present research started with the synthesis of ZrO₂ metal oxide by solution combustion (SCS) method using Zirconil nitrate with ODH as fuel best suited for reinforcing aluminium. The present work demonstrates that ZrO₂ reinforced aluminum can act and exhibit certain desirable properties relative to pure aluminum matrix. ZrO₂ nano particles are uniformly dispersed at 1 wt % dopant. 1 wt % is the most optimal value to resist the corrosion and increases the microhardness value to a maximum. Increasing trend in wear resistance of samples with increase in wt% of ZrO₂ shows that ceramic particles as nano-reinforcement can impart superior wear resistance to the host aluminum matrix. Metal oxide nano particles are very efficient at imparting their inherent properties to the host matrix like high hardness and strength since they have high surface area to volume ratio.

References

- [1] O. Zubillagaa, F.J. Canoa, I. Azkaratea, I.S. Molchanb, G.E. Thompsonb, P. Skeldonb. *Surface & Coatings Technology* 203 (2009) 1494–1501
- [2] J.R. Davis, *Corrosion of Aluminum and Aluminum Alloys*, First edition ASM International, USA, 1999.
- [3] C. Blanc, B. Lavella, G. Mankowski, *Corros. Sci.* 39 (3) (1997) 495.
- [4] V. Guillaumin, G. Mankowski, *Corros. Sci.* 41 (1999) 421.
- [5] P. Campestrini, H. Terryn, J. Vereecken, J.H.W. de Wit, *J. Electrochem. Soc.* 151 (6) (2004) B359.
- [6] P. Campestrini, H. Terryn, J. Vereecken, J.H.W. de Wit, *J. Electrochem. Soc.* 151 (6) (2004) B370.
- [7] M. Kendig, S. Jeanjaquet, R. Addison, J. Waldrop, *Surf. Coat. Technol.* 140 (2001) 58.
- [8] I. O Owate and E. Chukwuocha, *Scientific Research and Essay*. 3 (2007) 074-080.
- [9] A. I. Ogbonna, S. N. Asoegwu and P. C. Okebanama. *Journal of Corrosion Science and Technology*. 1 (2004) 135-146.
- [10] A. I. Onuchukwu, *Journal of Corrosion Science and Technology*. 2 (2004) 138-148.
- [11] O. Vasylykiv, Y. Sakka, *J. Am. Ceram. Soc.* 84 (2001) 2489.
- [12] V. Sergo, G. Pezzotti, O. Sbaizero, T. Nishida, *Act. Mater.* 46 (1998) 1701.
- [13] A. Heuer, L.W. Hobbs (Eds.), *Science and Technology of Zirconia*, *Advances in Ceramics*, vol. 3, American Ceramic Society, Westerville, OH, 1981; *Science and Technology of Zirconia II*, *Advances in Ceramics*, vol. 12, American Ceramic Society, Westerville, OH, 1984.
- [14] S. Somiya, N. Yamamoto, H. Yanagina (Eds.), *Advances in Ceramics*, vols. 24A and 24B, American Ceramic Society, Westerville, OH, 1988.
- [15] X. Zhao, D. Vanderbilt, *Phys. Rev. B* 65 (2002) 075105.
- [16] E.J. Walter, S.P. Lewis, A.M. Rappe, *Surf. Sci.* 495 (2001) 44.
- [17] J. Zhu, M.S.M.M. Rahuman, J.G. van Ommen, L. Lefferts, *Appl. Catal. A* 259 (2004) 95.
- [18] J. Zhu, J.G. van Ommen, L. Lefferts, *J. Catal.* 225 (2004) 388.
- [19] J. Zhu, Ph.D. Thesis, University of Twente, The Netherlands, 2005.
- [20] J. Zhu, J.G. van Ommen, J.G. Knoester, L. Lefferts, *J. Catal.* 230 (2005) 291.
- [21] J. Zhu, S. Alberstsma, J.G. van Ommen, L. Lefferts, *J. Phys. Chem. B* 109 (2005) 9550.
- [22] S. Meriani, *Zirconia'88: Advances in Zirconia Science and Technology*, Elsevier, New York, 1989.
- [23] C.B. Alcock, *Mater. Sci. Res.* 10 (1975) 419.
- [24] F.J. Rohr, *Solid Electrolytes*, *Material Science Series*, Academic, New York, 1978.

- [25] A. Meldrum, L.A. Boatner, R.C. Ewing, *Phys. Rev. Lett.* 88 (2002) 025503.
- [26] C. Morant, J.M. Sanz, L. Galán, *Phys. Rev. B* 45 (1992) 1391.
- [27] V. Fiorentini, G. Gulleri, *Phys. Rev. Lett.* 89 (2002) 266101.
- [28] R. Punthenvilakam, E.A. Carter, J.P. Chang, *Phys. Rev. B* 69 (2004) 155329.
- [29] D. Wang, G.P. Bierwagen, *Prog. Org. Coat.* 64 (2009) 327.
- [30] M. Fallet, H. Mahdjoub, B. Gautier, J.P. Bauer, *J. Non Cryst. Solids* 293–295 (2001) 527.
- [31] M. Guglielmi, D. Festa, P.C. Innocenzi, P. Colombo, M. Gobbin, *J. Non-Cryst. Solids* 147–148 (1992) 474.
- [32] G. Ruhi, O.P. Modi, I.B. Singh, A.K. Jha, A.H. Yegneswaran, *Surf. Coat. Technol.* 201 (2006) 1866.
- [33] H. Li, K. Liang, L. Mei, S. Gu, S. Wang, *Mater. Lett.* 51 (2001) 320.
- [34] H. Li, K. Liang, L. Mei, S. Gu, S. Wang, *J. Mater. Sci. Lett.* 20 (2001) 1081.
- [35] H. Li, K. Liang, L. Mei, S. Gu, *Mater. Sci. Eng. A* A341 (2003) 87.
- [36] M.A. Domínguez-Crespo, A. García-Murillo, A.M. Torres-Huerta, F.J. Carrillo-Romo, E. Onofre-Bustamante, C. Yáñez-Zamora, *Electrochim. Acta* 54 (2009) 2932.